Iranian Journal of Hydrogen & Fuel Cell 3(2014) 141-152

Iranian Journal of Hydrogen & Fuel Cell

IJHFC

Journal homepage://ijhfc.irost.ir

The effect of inclined radial flow in proton exchange membrane fuel cells performance

F. Ramin [1], A.Torkavannejad[2,*], S. Baheri [1]

[1] Department of Mechanical Engineering, University of Tabriz, Postal Code 57531-12331,Tabriz, Iran [2] Department of Mechanical Engineerin, University of Urmia, Postal Code 57561-15311, Urmia, Iran

Article Information

Article History:

Received:
12 August 2014
Received in revised form:
11 November 2014
Accepted:
17 November 2014

Keywords

Fuel cell performance
PEM fuel cells
Single-phase
Radial channel flow

Abstract

Computational fluid dynamics analysis was employed to investigate the radial flow field patterns of proton exchange membrane fuel cells (PEMFC) with different channel geometries at high operating current densities. A 3D, non- isothermal model was used with single straight channel geometry. Our study showed that new generation of fuel cells with circle stack with the same active area and inlet area gave higher current density compared with conventional model. The main factors that affect the behavior of each of the curves are discussed. Species and temperature contours are presented for the new model, showing how the fuel cell behavior is affected by species penetration due to increasing inlet and outlet in one mono cell (four inlet and out let) with inclined in the radial channel configuration.Velocity trends are presented for the two different models, showing how the fuel cell behavior is affected by the velocity variations in the radial configuration. Thus, the results presented here suggest that the radial geometry is a strong candidate for the near-future development of the fuel cell technology.

1. Introduction

Fuel cells are electrochemical devices that change chemical energy of reactants, directly into electrical energy. The important features of fuel cell that sharply increased the appeal of fuel cells in generating electricity include: high performance, not being limited to Carnot cycle, silent and long term operation, and not having problems of emission control and waste disposal. These advantages make the fuel cells attractive choices for the replacement to internal combustion engines [1]. High cost of launch and economical cost is the major disadvantages of fuel cells. Different types of fuel cells have been developed, which are distinguished by the electrolyte used. Among all kinds of fuel cells, proton exchange membrane fuel cell (PEMFC) has been considered as a principle candidate for future transportation application as well as for small devices such as laptop. In these fuel cells, fuel (e.g., hydrogen gas) and an oxidant (e.g., oxygen gas from the air) are used to generate electricity, while heat and water are

*Corresponding author: a.torkavannejad@urmia.ac.ir

unavoidable products of the fuel cell operation. A fuel cell typically works on the following principle: as the hydrogen gas flows into the fuel cell on the anode side, a platinum catalyst facilitates oxidation of the hydrogen gas which produces protons (hydrogen ions) and electrons. The hydrogen ions diffuse through MEA. The electrons, which cannot pass through the membrane, flow from the external electrical circuit for energy consumption. At the cathode side, oxygen molecules combine with hydrogen ions and produce water and heat. The anode and the cathode (the electrodes) are porous and made of an electrically conductive material, typically carbon. The PEM electrodes are generally designed for maximum surface area per unit material volume.
In recent years, researchers pay more attention to modeling and simulation of different aspects in PEMFCs with a view to enhance the cell performance and optimize the cost. In this way, a great number of researches have been conducted to improve the performance of PEMFC. Among these studies, various operating condition have been examined [2-10]. Another major issue that researchers focus more for commercialization of these cells, is the geometrical design of PEMFC. One of the geometrical parameters that affect the fuel cells is the shoulder width. It has been found that cells with smaller shoulder width are better than those with larger shoulder width due to more uniform distribution of reactants [11-15]. Other geometries have been investigated to increase permeability of reactants by using obstacle in channel area [16] and different channel geometries [17-20]. Various serpentine flow fields have been examined for reaching higher output [21-24]. D.H. Ahmed et al [25] performed simulations of PEMFCs with a new design for the channel shoulder geometry, in which the MEA is deflected from shoulder to shoulder. F. Arabi et al. investigated the effect of an innovative bipolar plate on PEMFC performance [26]. In the previous years, researchers pay more attention on the new geometries like radial and spiral flow PEMFCs for the sake of performance enhancement [27-31].
In the present study, a three-dimensional, single phase, non-isothermal and parallel flow model of a PEM fuel cell with radial channel was performed which channel inclined in both anode and cathode toward gas diffusion layer for more diffusion. These geometries were used the same boundary conditions and inlet area and including humidification for both anode and cathode. This new geometry was designed to improve the reactant distribution and improve the cell performance.
The simulation results were validated by comparison with results in the literature and showed good concord with experimental data. Detailed analyses of the fuel cell behavior under this generation of channels are discussed in the following sections.

2. Model description

2.1. System description

Constant mass flow rate at the channel, inlet constant pressure condition at the channel outlet, and no-flux conditions are executed for mass, momentum, species and potential conservation equations at all boundaries expect for inlets and outlets of the anode and cathode flow channels. The side's faces are symmetrical.
Figure 1 indicates the traditional domain of base model and table 1 shows the Geometric parameters and operation conditions for base model [32]. The cell consists of hydrogen and oxygen channels, bipolar plates on cathode and anode side of cell, which act as current collector with high electronic conductivity and the membrane electrode assembly (MEA) is located between gas channels.

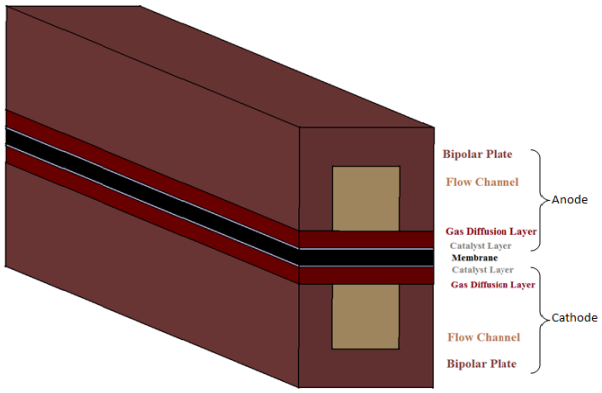

Fig. 1. Computational domain of the model

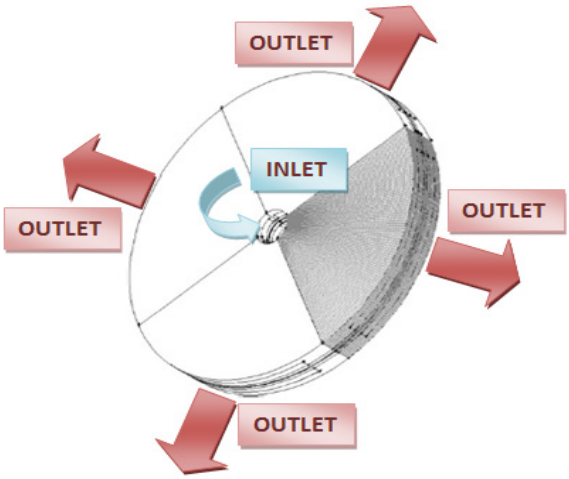

Fig. 2. Schematic of the radial fuel cell

2.2. Model assumptions

A non-isothermal model is assumed to perform in steady manner. All gases are assumed to obey ideal gas behaviors. Gas diffusion and catalyst layers are considered to be homogeneous and isotropic porous mediums. Flow is incompressible and laminar due to the low pressure gradients and velocities. Volume of liquid-phase water produced in electrochemical reactions is negligible and phase change or two phase-transports are not considered so this model is considered as a single phase. The membrane is impermeable to cross-over of reactant gases and assumed to be fully humidified. The species diffusion and electrochemical reaction conform to the dilute solution theory and Butler-Volmer kinetic equation, respectively.

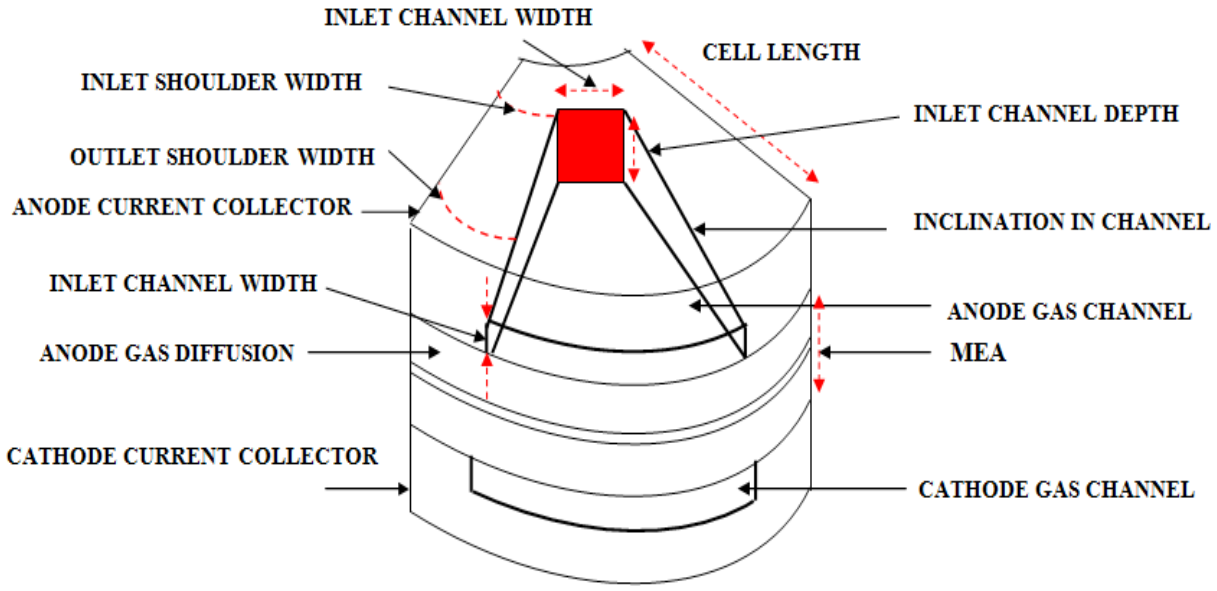

Fig. 3. Simplified model of the radial fuel cell

Figure 2 and 3 show the configuration of the proposed fuel cell. This fuel cell has the same active and operation condition which the base fuel has, in order to compare the result. The reactant gases are supplied from inlet channels and leaved by the area formed in the outer edge of the cell. This new geometry is very unique and novel due to its geometry and performance. The geometric parameters are presented table 2.

3. Model equations

3. 1. Gas flow fields

In the fuel cell, the gas-flow field is obtained by solving the steady-state Navier-Stokes equations, i.e.

$$\Delta.\left(\rho u\right)=0 \tag{1}$$

And momentum equations;

$$\nabla.\left(\rho u\otimes u-\mu\nabla u\right)= -\nabla\left(P+\frac{2}{3}\mu\nabla u\right)+\nabla.\left[\mu\left(\nabla u\right)^{T}\right] \tag{2}$$

The mass balance is described by the divergence of the mass flux through diffusion and convection. The steady state mass transport equation can also be written in the following expression for species i;

$$\nabla\left[-\rho y_i\sum_{j=1}^{N}D_{ij}\frac{M}{M_j}\left(\nabla y_j+y_j\frac{\nabla M}{M}\right)+\rho y_i u\right]=0 \tag{3}$$

Where the subscript i denotes oxygen at the cathode side and hydrogen at the anode side, and j is water vapor in both cases. Nitrogen is the third species at the cathode side.

The Maxwell-Stefan diffusion coefficients of any two species are dependent on temperature and pressure. They can be calculated according to the empirical relation based on the kinetic gas theory [32];

$$D_{ij}=\frac{T^{1.75}\times10^{-3}}{P\left[\left(\sum_k V_{ki}\right)^{1/3}+\left(\sum_k V_{kj}\right)^{1/3}\right]^2}\left[\frac{1}{M_i}+\frac{1}{M_j}\right]^{1/2} \tag{4}$$

In this equation, pressure is in [atm], and the binary diffusion coefficient is in [cm^2/s]. The values for $\sum V_{ki}$ are given by Fuller et al. [32], and the temperature field is obtained by solving the convective energy equation;

$$V.\left(\rho C_p uT-kVT\right)=0 \tag{5}$$

3. 2. Gas diffusion layers

Transport in the gas diffusion layer is modeled as transport in a porous media. The continuity equation in the gas diffusion layers becomes:

$$\nabla.\left(\rho\varepsilon u\right)=0 \tag{6}$$

The momentum equation reduces to Darcy's law:

$$u=\frac{K_p}{\mu}\nabla P \tag{7}$$

The mass transport equation in porous media is:

$$\nabla.\left[-\rho\varepsilon y_i\sum_{j=1}^{N}D_{ij}\frac{M}{M_j}\left(\nabla y_j+y_j\frac{\nabla M}{M}\right)+\rho\varepsilon y_i u\right]=0 \tag{8}$$

In order to account for geometric constraints of the porous media, the diffusivities are corrected using the Bruggemann correction formula:

$$D_{ij}^{eff}=D_{ij}\times\varepsilon^{1.5} \tag{9}$$

The heat transfer in the gas diffusion layers is governed by:

$$\nabla.\left(\rho\varepsilon C_p uT-k_{eff}\varepsilon\nabla T\right)=\varepsilon\beta\left(T_{solid}-T\right) \tag{10}$$

Where, the term on the right- hand side accounts for the heat exchange to and from the solid matrix of the GDL. Here β is a modified heat transfer coefficient that accounts for the convective heat transfer in [W/m^2] and the specific surface area [m^2/m^3] of the porous medium [32]. Hence, the unit of β is [W/m^3]. The potential distribution in the gas diffusion layers is:

$$\nabla.\left(\lambda_e\nabla\phi\right)=0 \tag{11}$$

3.3. Catalyst layers

The catalyst layer is treated as a thin interface, where sink and source terms for the reactants are implemented. Due to the infinitesimal thickness, the source terms are actually implemented in the last grid cell of the porous medium. At the cathode side, the sink term for oxygen can be written as:

$$S_{O_2} = -\frac{M_{O_2}}{4F} i_c \quad (12)$$

Whereas the sink term for hydrogen is specified as:

$$S_{H_2} = -\frac{M_{H_2}}{4F} i_a \quad (13)$$

The production of water is modeled as a source terms and hence can be given as:

$$S_{H_2O} = -\frac{M_{H_2O}}{2F} i_c \quad (14)$$

The generation of heat in the cell is due to entropy changes as well as irreversibility due to the activation over potential:

$$\dot{q} = \left[\frac{T(-\nabla s)}{n_e F} + \eta_{act,c} \right] i_c \quad (15)$$

The local current density distribution in the catalys layers can be modeled by the Butler-Volmer equation:

$$i_c = i_{o,c}^{ref} \left(\frac{C_{O_2}}{C_{O_2}^{ref}} \right) \left[\exp\left(\frac{\alpha_a F}{RT} \eta_{act,c} \right) + \exp\left(-\frac{\alpha_c F}{RT} \eta_{act,c} \right) \right] \quad (16)$$

$$i_a = i_{o,a}^{ref} \left(\frac{C_{H_2}}{C_{H_2}^{ref}} \right) \left[\exp\left(\frac{\alpha_a F}{RT} \eta_{act,a} \right) + \exp\left(-\frac{\alpha_c F}{RT} \eta_{act,a} \right) \right] \quad (17)$$

3. 4. Membrane

The balance between the electro-osmotic drag of water from anode to cathode and back diffusion from cathode to anode yields the net water flux through the membrane:

$$N_w = n_d M_{H_2O} \frac{i}{F} - \nabla\left(pD_w \nabla y_w \right) \quad (18)$$

For heat transfer purposes, the membrane is considered a conducting solid, which means that the transfer of energy associated with the net water flux through the membrane is neglected. Heat transfer in the membrane is governed by:

$$\nabla.\left(K_{mem} \nabla T \right) = 0 \quad (19)$$

The potential loss in the membrane is due to resisting to proton transport across membrane which is equal to:

$$\nabla.\left(\lambda_m \nabla \phi \right) = 0 \quad (20)$$

3. 5. Boundary conditions

For the momentum conservation equation, fuel velocity is specified at each inlet of anode and cathode flow channel. The velocity is calculated based on the concept of stoichiometry. Boundary conditions are set as follows: constant mass flow rate at the channel inlet and constant pressure condition at the channel outlet which means it discharges to the atmosphere. The inlet mass fractions are determined by the inlet pressure and humidity according to the ideal gas law. Gradients at the channel exits are set to zero. The equations for both inlets are expressed as:

$$\left| \vec{u} \right|_{in} = \frac{\zeta}{X_{H_{2,in}}} \frac{I_{avg}}{2F} \frac{RT_{in}}{P_{in}} \frac{A_{MEA}}{A_{ch}} \quad (21)$$

I_{avg} is the average current density at a given cell-potential. Where, R, T_{in}, P_{in}, and ζ are the universal gas constant, temperature at the inlet, pressure at the inlet, and stoichiometric ratio, respectively. The later is defined as the ratio between the amount of supplied and the amount of required reactants on the basis of the reference current density I_{avg} , accordingly. The model parameter values are given in Tables 1 and 2, and the inlet conditions are shown in Table 1. The electrode-membrane parameters obtained from Ref. [31].

4. Numerical implementations

For solving the equations, the computational fluid dynamic codes are used by applying simple algorithm. In addition the main procedure for discretizing the governing equations with the appropriate boundary conditions is finite volume method. Figure 4 shows the algorithm (SIMPLE) with finite volume for solving model equations which is a constant and routine method. A grid independence test results were performed to ensure that the solutions were independent of the grid size. Moreover, the computational domain is divided into about 164000 unstructured cells to minimize the numbers of iteration and maximizing the accuracy.

The number of calculation was used as 500 for low current density and 900 for high current density and the criterion convergence is less than 10^{-6} for all variables. An IBM-PC-Pentium 5 (CPU speed is 2.4GHz) was determined to solve the set of equations. The computational time for solving the set of equations was 6 h.

Table 1. Geomerric paramets and operation conditions for base model.

Parameter	Symbol	Value	Unit
Channel length	L	0.05	m
Channel width	W	1e_3	m
Channel height	H	1e_3	m
Land area width	Wland	1e_3	m
Gas diffusion layer thickness	dGDL	0.26e_3	m
Wet membrane thickness (Nafion 117)	memδ	0.23e_3	m
Catalyst layer thickness	CLδ	0.0287e_3	m
Anode pressure	Pa	3	atm
Cathode pressure	Pc	3	atm
Inlet fuel and air temperature	Tcell	353.15	K
Relative humidity of inlet fuel and air (fully humidified conditions)	ψ	100	%
Refrence current density	I	10	A/cm^2
Inlet anode oxygen mass fraction	$Y_{OXYGEN,A}$	0	-
Inlet anode hydrogen mass fraction	$Y_{HYDROGEN,A}$	0.3780066	-
Inlet anode water mass farction	$Y_{WATER,A}$	0.6219934	-
Inlet cathode water mass fraction	$Y_{WATER,C}$	0.1031307	-
Inlet cathode oxygen mass fraction	$Y_{OXYGEN,C}$	0.2088548	-
Inlet carhode hydrogen mass fraction	$Y_{HYDROGEN,C}$	0	-
Membrane equivalent weight	-	1.1	Kg/mol

Table 2. Geometric parametrs for simplified model (single cell)

Inlet channel depth	1 mm
outlet channel depth	0.25 mm
Inlet channel Width	1 mm
Arc of inlet curvature for the simplified model	1 mm
Arc of outlet curvature for the simplified model	3 mm
Cell length	5.64 mm
inlet shoulder width	0.28 mm
Outlet shoulder width	1.4 mm

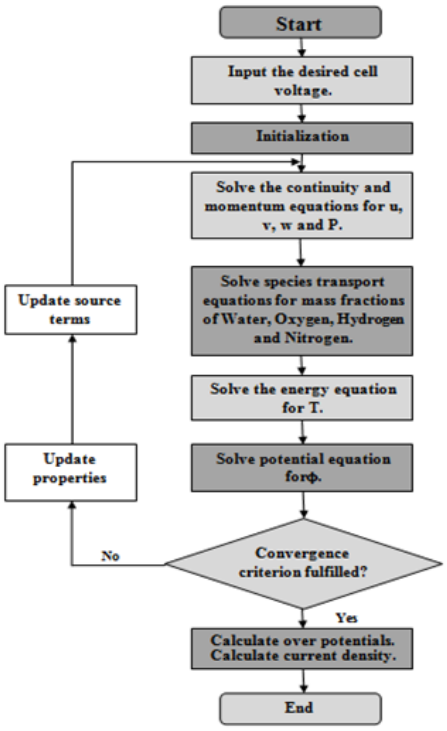

Figure 4.The algorithm for numerical simulation.

5. Results and discussions

To validate the numerical simulation model used in the present study, the polarization curves were compared with the experimental data presented by Al-Baghdadi et al for straight channel [32]. Polarization curve of present model is shown in Figure 5. This curve signifies excellent agreement between numerical model results and experimental data. The Proposed model (the model with four channels) was chosen with the same reactant flow rate and constant boundary conditions. The fully humidified inlet condition for anode and cathode was used. Parametric and operating conditions can be found in Table 1 [32]. In order to improve conventional cell performance by improving the distribution of reactants over the GDL, we simulated radial flow pattern. The comparison

of the cell performance of the geometry proposed

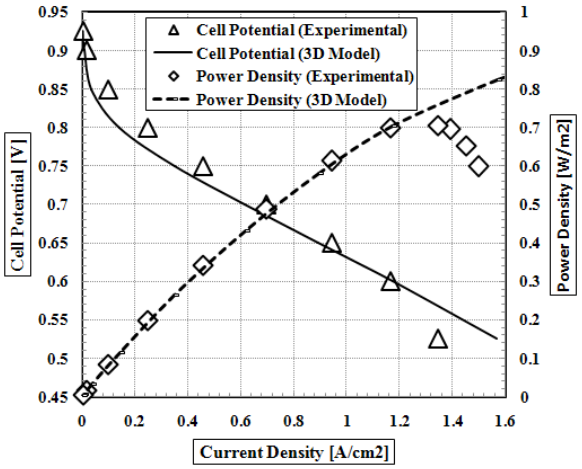

Figure 5.Polarization curve of Base model.

in this work with fuel cells with a conventional flow field must be done via polarization curves. The figure 6 revealed that case with radial flow produces more current density than the conventional geometry produces. As shown in Figures 7 and 8, the radial model performance and current density is more than conventional geometry. The figure demonstrates that in the radial flow model can get the highest value of current density. [30, 33].

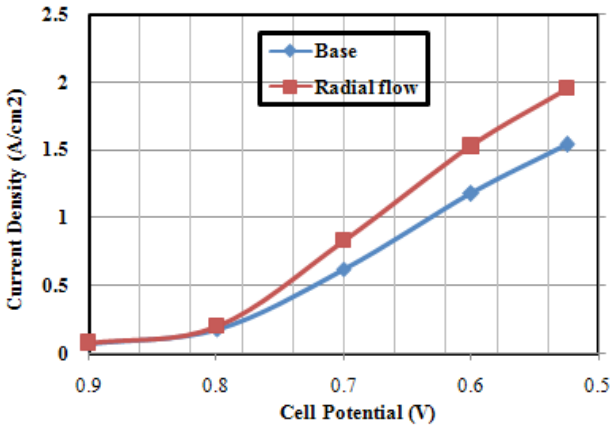

Figure 6. Comparison of performance of two numerical cases.

Figure 9 shows the profile of oxygen distribution at the membrane-cathode catalyst interface which is obtained at 0.6 volt. Since the simplified model shows (figure 3), inclining the channels causes decreasing outlet channel area in order to increase the momentum of species molecules for better diffusion. More gases forced into and passing through the gas diffusion layer

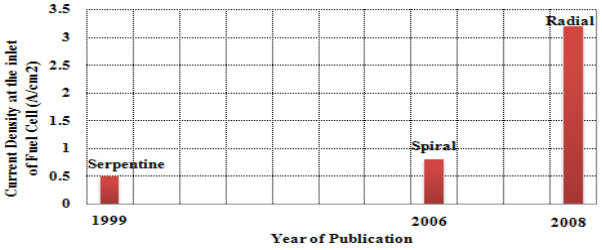

Figure 7. Maximum current density for the radial model compared with the conventional serpentine and spiral geometries[33].

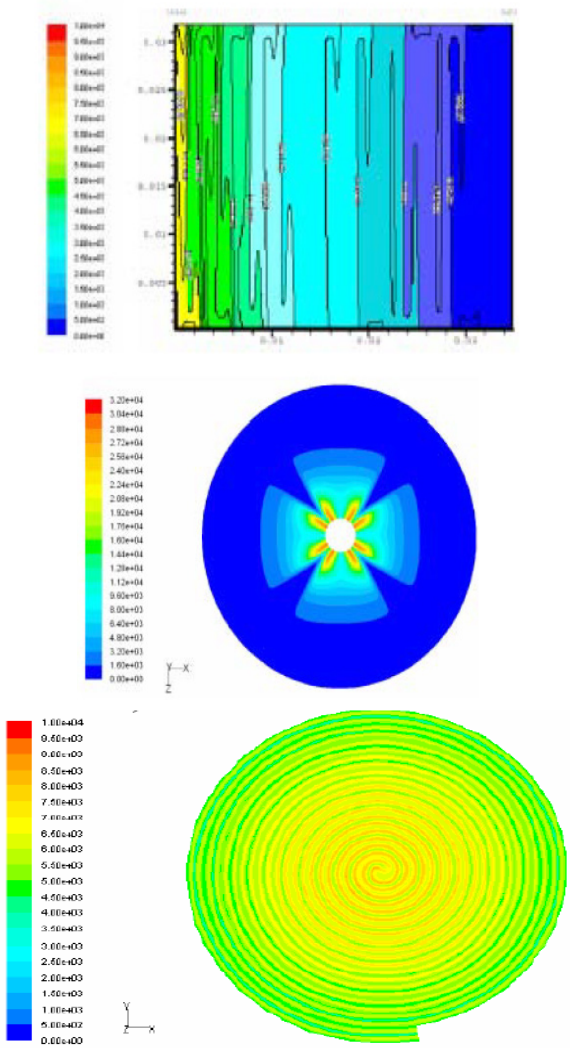

Figure 8: Current density contours for a fuel cell channel configuration of: (a) serpentine, (b) radial, (c) Archimedes spiral [30].

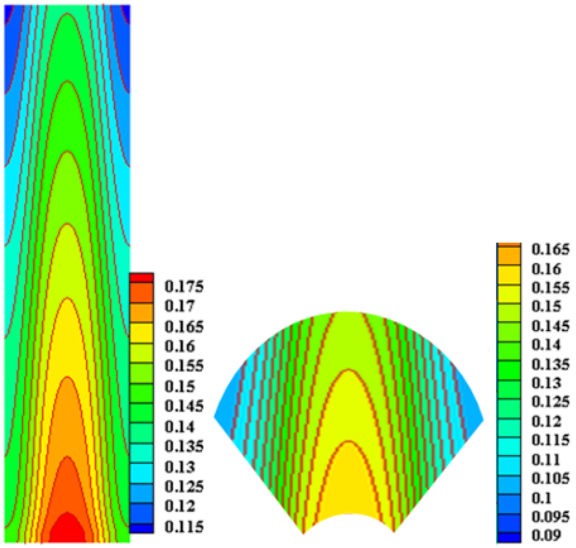

Figure 9. Contours of oxygen mole fraction at the cathode interface of catalyst and gas diffusion layer of cathode for the base and radial flow (0.6 volt).

as presented in Figure 10. Results show the mass fraction of the oxygen increase as the inclination increases in outer region of cathode in comparison with base model. As a result, a more uniform profile for the oxygen concentration is read when using new geometry.

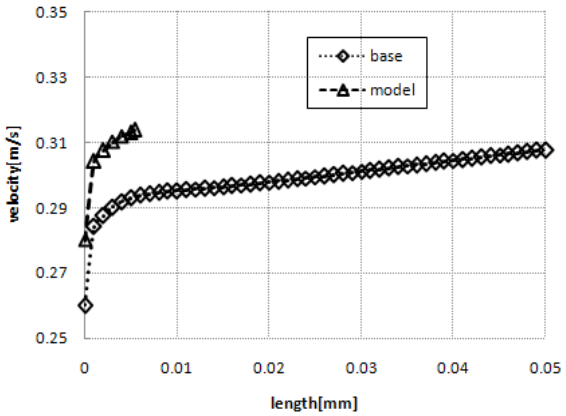

Figure 10. trend of velocity magnitude along the cathode channel for the base and radial flow (0.6 volt).

The water molar fraction distribution in the cell is shown in Figure 11 at V = 0.6 V for two geometries. As shown in Fig. 9, water molar fraction increases along the channel due to the water production by oxygen consumption at the catalyst layer and the net water transfer from the anode side through the membrane toward the cathode side. Water has deterministic role

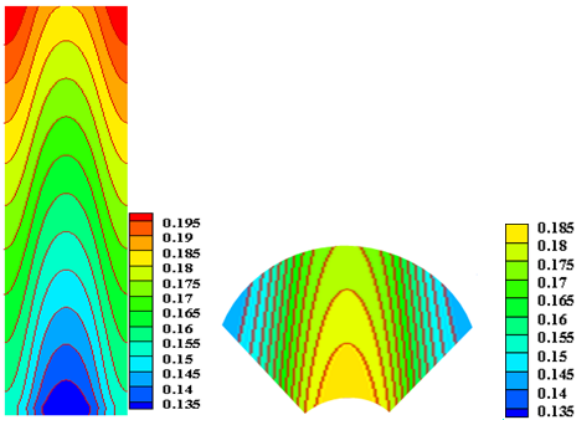

Figure 11. Contours of water mole fraction at the cathode interface of catalyst and gas diffusion layer for the base and radial flow (0.6 volt).

on the PEMFC performance, additionally, any variation in water causes dehydration or flooding of PEMFC which must be controlled during performance the fuel cell.

It can be obtained in the downstream of channel the amount of water increases due to generating water molecules, which is uniform along the channel. It is found that the geometry presented in this work can be good option against removing water due to have four outlets and short channel.

Figure 12 shows the influence of the internal flow modification on the distribution of temperature at 0.6. cell voltage for radial flow between GDL and catalyst plate. It is clear that the temperature gradually increases along the cell because of moving the more fuel gas into the gas diffusion layer to enhance the chemical reaction at the catalyst layer. It can be seen that the maximum temperature of the cell is at the cathode catalyst layer that it is due to the maximum heat generation at the cathode side catalyst layer. Also Figure 12 shows a depression region around the location of the connections between GDL and bipolar plate. This depression region is caused by increasing the traversed distance of gases on the surface, which decreases the temperature of them and formation more water vapor at this region and condensation of them.

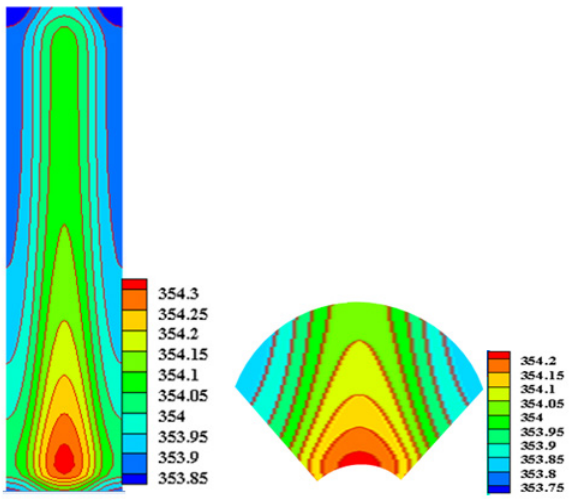

Figure 12. Contours of Temperaure at the cathode interface of catalyst and gas diffusion layer for the base and radial flow (0.6 volt).

6. Conclusion

In the present work, a three-dimensional computational fluid dynamics model of PEMFC with radial inclined flow channel has been simulated in order to improve the cell performance. An important result is the higher current density which obtained in this unconventional model. it is found that the geometry presented in this work is capable of producing large current densities when the whole cell is considered.

The efficacy of this geometry was studied compared with base model while the inlet area and boundary conditions have been considered constant for all cases. The species distribution and the performance of all models, such as polarization curve, oxygen and Water and temperature counters have been studied. Additionally, the numerical results showed that reactants distribute more uniformly compared with the base model. The performance of this radial model could be improved by inclining flow channel and increasing the species velocity. At the mid of channel due to increasing the channel area inclination of channel giving the species molecules have the necessary momentum to avoid stagnation (and avoid flooding), and resulting in a more homogeneous current density distribution. Radial flow seems to be better option, because the physical removal of water is easier as there are four outlets instead of one and facilitate the penetration of species.

The favorable results obtained for this unique work seems to indicate that this geometry could replace the conventional commercial geometries currently in use. Future work will be to build and manufacture the geometriy proposed and compare all of them experimentally

7. Acknowledgment

The financial support of the Renewable Energy Organization of Iran is gratefully acknowledged (SUNA).

Nomenclature:

A	superficial electrode Area (m^2)
C	molar concentration (mol m^{-3})
a	Water activity
D	Mass diffusion coefficient (m^2/s)
F	Faraday constant (C/mol)
I	Local current density (A/m^2)
J	Exchange current density (A/m^2)
K	Permeability (m^2)
M	Molecular weight (kg/mol)
nd	Electro-osmotic drag coefficient
P	Pressure (Pa)
S	stoichiometric ratio
R	Universal gas constant (J/mol.K)
T	Temperature (K)
t	Thickness
V	Cell voltage
Voc	Open-circuit voltage
W	Width
X	Mole fraction

Greek letters:

α	Water transfer coefficient

ε_{eff}	Effective porosity
ρ	Density (kg/m^3)
μ	Viscosity (kg/m-s)
σ_e	Membrane conductivity (1/ohm-m)
λ	Water content in the membrane
ζ	Stoichiometric ratio
η	Over potential (v)
λ_{eff}	Effective thermal conductivity (w/m-k)

Subscripts and superscripts:

a	Anode
c	Cathode
cl	Catalyst
GDl	Gas diffusion layer
ch	Channel
k	Chemical species
m	Membrane
MEA	Membrane electrolyte assembly
ref	Reference value
sat	saturated
w	Water

8. References

[1] Mardi Kolur, M. Khalil Arya, S., Jafarmadar, S. and Nemati, A., Hydrgen and ethanol as potential alterbative fuel compared to gasoline under improved exhaust gas recirculation. Journal of International of engineering. 27, No. 3 (March 2014) 449-456.

[2] Xing et al., Optimization of assembly clamping pressure on performance of proton-exchange membrane fuel cells, J.Power Sources, 195 (2010) 62-68.

[3] Chang et al., Effect of clamping pressure on the performance on a PEM fuel cell, J. Power Sources, 166 (2007) 149-154.

[4] Rho, Y. W., Velev, O. A., Srinivasan, S., and Kho, Y. T., Mass transport in proton exchange membrane fuel cells usingO_2/H_2, O_2/Ar, and O_2/N_2 mixtures, J. Electrochem. Soc.,141.

[5] Amphlett, J. C., Baumert, R. M., Mann .R. F., Peppley, B. A., Roberge, P. R. and Harris, T. J., Performance modeling of the ballard mark IV solid polymer electrolyte fuel cell. I.

[6] Mosdale, R., and Srinivasan, S., Analysis of performance and of water management in proton exchange membrane fuel cells, Electrochem. Acta, 40 (1995) 413-421.

[7] Oetjen, H.-F., Schmidt, V. M., Stimming, U. and Trila, F., Performance data of a proton exchange membrane fuel cell using H2/Co as fuel gas, J. Electrochem.Soc., 143 (1996) 38-42.

[8] Buchi, F. N., and Srinivasan, D., Operating proton exchange membrane fuel cells without external humidification of the reactant gases, J. Electrochem. Soc., 144 (1997) 27-67.

[9] Uribe, F. A., Gottesfeld, S. and Zawodzinski, T. A., Effect of ammonia as potential fuel impurity on proton exchange membrane fuel cell performance, J. Electrochem. Soc., 149 (2002) A293.

[10] Ticianelli, E. A., Derouin, C. R. and Srinivasan, S., Localization of platinum in low catalyst loading electrodes to attain high power densities in SPE fuel cells, J. Electro anal.Chem., 251 (1988) 275.

[11] Natarajan, D. T., Nguyen, V., A two-dimensional, two-phase, multicomponent, transient model for the cathode of a proton exchange membrane fuel cell using conventional gas distributors, J. Electrochem. Soc. 148 (12) (2001) 1324–1335.

[12] Lin, G., Nguyen. T.V., A two-dimensional two-phase model of a PEM fuel cell. J. Electrochem. Soc. 153 (2) (2006) 372–382.

[13] Lum, K.W., McGuirk, J.J., Three-dimensional model of a complete polymer electrolyte membrane fuel cell – model formulation, validation and parametric studies, J. Power Sour. 143(2005) 103–124.

[14] Ahmed, D.H., Sung, H.J., Effects of channel

geometrical configuration and shoulder width on PEMFC performance at high current density, J. Power Sour. 162 (2006) 327–339.

[15] Torkavannejad, A., pesteei, m., Ramin, F., Ahmadi, N., Effect of innovative channel geometry and its effect o species distribution in PEMFC, journal of renewable energy and environment, Volume 1 - 1, January 2014, pp. 20-31

[16] Torkavannejad, A., pourmahmood, N., Mirzaee, I., Ramin, F., effect of gas flow channel on the performance of proton Exchenge Membrane fuel cell, Indian journal of scientific research, 4 (5): 619-632, 2014.

[17] Ahmadi, N., Rezazadeh, S., Mirzaee, I., and Pourmahmoud, N., Three-dimensional computational fluid dynamic analysis of the conventional PEM fuel cell and investigation of prominent gas diffusion layers effect. Journal of Mechanical Science and Technology .12(8) (2012) 1-11.

[18] Ge, S., and Yi, B., A Mathematical Model for PEMFC in Different Flow Modes. Journal of Power Sources, 124(1) (2003) 1-11.

[19] Sun, L., Oosthuizen, P.H. and McAuley, K.B., A Numerical Study of Channel-to-Channel Flow Cross-over Through the Gas Diffusion Layer in a PEM-fuel-cell Flow System Using a Serpentine Channel with a Trapezoidal Cross-sectional Shape. International Journal of Thermal Sciences, 45(10) (2006) 1021-1026.

[20] Guvelioglu, G.H., Stenger, H.G., Computational Fluid Dynamics Modeling of Polymer Electrolyte Membrane Fuel Cells. Journal of Power Sources, 147(9) (2005) 95-106.

[21] Chiang, M.S., and Chu, H.S., Numerical Investigation of Transport Component Design Effect on a Proton Exchange Membrane Fuel Cell. Journal of Power Sources, 160(1) (2006) 340-352.

[22] Shimpalee, S. W., Lee, K., Van Zee, J.W., Neshat, H.N., Predicting the transient response of a serpentine flow-field PEMFC I. Excess of normal fuel and air, J. Power Sources 156 (2) (2006) 355–368.

[23] Weng, F.B., Su, A., Jung, G.B., Chiu, Y.C., Chan, S.H., Numerical prediction of concentration and current distribution in PEMFC. J. Power Sources 145(2005) 546–554.

[24] Su, A., Chiu, Y.C., Weng, F.B., The impact of flow field pattern on concentration and performance in PEMFC. Int. J. Energy Res. 29(2005) 409–425.

[25] Ahmed, D.H., Sung, H.J., Designs of a deflected membrane electrode assembly for PEMFCs, J. Heat and Mass Transfer. 51(2008) 327–339.

[26] Arabi, A. and Roshandel, R.,Numerical modeling of an innovative bipolar plates design based on the leaf venation patterns for PEM fuel cells. International journal of engineering, 25-3 (2012) 177-186.

[27] S. Cano-Andrade, A. Hernandez-Guerrero, M.R. von Spakovsky , C.E. Damian-Ascencio, J.C. Rubio-Arana, “Current density and polarization curves for radial flow field patterns applied to PEMFCs (Proton Exchange Membrane Fuel Cells), Energy 35 (2010) 920–927.

[28] B.R. Friess, M. Hoorfar, “Development of a novel radial cathode flow field for PEMFC”, International Journal of hydrogen energy, 37 (2012), 7719-7729.

[29] Surajudeen Olanrewaju Obayopo, “Performance Enhancement in Proton Exchange Membrane Fuel Cell-Numerical Modeling and Optimisation”, PhD thesis, University of Pretoria, 2012.

[30] “Three Dimensional Analysis of a PEM Fuel Cell with the Shape of a Fermat Spiral for the Flow Channel Configuration”, Proceedings of IMECE2008, ASME International Mechanical Engineering Congress and Exposition October 31-November 6, 2008, Boston, Massachusetts, USA.

[31] Brooks Regan Friess, “Development of Radial Flow

Channel for Improved Water and Gas Management of Cathode Flow Field in Polymer Electrolyte Membrane Fuel Cell", Masters of Applied Science Thesis, University of British Columbia, 2010.

[32] Maher A.R. Sadiq Al-Baghdadi, Haroun A.K. Shahad Al-Janabi, "Parametric and optimization study of a PEM fuel cell performance using three-dimensional computational fluid dynamics model", Renewable Energy 32 (2007) 1077–1101.

[33] S. Cano-Andrade, A. Hernandez-Guerrero, M.R. von Spakovsky b, C.E. Damian-Ascencio, J.C. Rubio-Arana, "Current density and polarization curves for radial flow field patterns applied to PEMFCs (Proton Exchange Membrane Fuel Cells), Energy 35 (2010) 920–927.".